IAC-08- C1.3.10

On the Consequences of a Fragmentation Due to a NEO Mitigation Strategy

J.P. Sanchez
University of Glasgow, Glasgow, United Kingdom,
psanchez@aero.gla.ac.uk
M. Vasile
University of Glasgow, Glasgow, United Kingdom,
m.vasile@aero.gla.ac.uk
G. Radice
University of Glasgow, Glasgow, United Kingdom,
gradice@aero.gla.ac.uk

ABSTRACT

The fragmentation of an Earth threatening asteroid as a result of a hazard mitigation mission is examined in this paper. The minimum required energy for a successful impulsive deflection of a threatening object is computed and compared with the energy required to break-up a small size asteroid. The fragmentation of an asteroid that underwent an impulsive deflection such as a kinetic impact or a nuclear explosion is a very plausible outcome in the light of this work. Thus a model describing the stochastic evolution of the cloud of fragments is described. The stochasticity of the fragmentation is given by a Gaussian probability distribution that describes the initial relative velocities of each fragment of the asteroid, while the size distribution is expressed trough a power law function. The fragmentation model is applied to Apophis as illustrative example. If a barely catastrophic disruption (i.e. the largest fragment is half the size the original asteroid) occurs 10 to 20 years prior to the Earth encounter only a reduction from 50% to 80% of the potential damage is achieve for the Apophis test case.

1. INTRODUCTION

THE threat that asteroids pose to life on Earth has for long been acknowledged [1]. Many techniques to deviate threatening asteroids have been proposed in the last three decades. Some of these techniques propose the application of a very low acceleration on the asteroid, while others use a high speed impact or an explosion to produce an impulsive change in linear momentum. If an impulsive deviation technique is applied to an asteroid, and the energy delivered by the deviation method is above a limit threshold [2; 3], a catastrophic fragmentation, i.e., fragmentation such that the largest fragment contains less than half the mass of the original asteroid, is likely to occur.

Plenty of studies have classified, evaluated and compared the existing techniques in terms of deviation efficiency [4-8], but little has been done on the analysis of a possible fragmentation[9]. This paper examines the consequences of a catastrophic fragmentation due to an impulsive deviation strategy. In particular, we consider the minimum level of energy (collisional energy) required to deviate an asteroid by a distance that ensures a successful deflection, even considering the hyperbolic trajectory that the asteroid will follow when approaching the Minimum Orbit Interception Distance (MOID) from the Earth. This minimum level of collisional energy is strongly dependent on the warning time or time available before the impact of the asteroid with the Earth. The collisional energy is then compared with the predicted specific energy required to

1

completely fracture the asteroid. As will be shown in the paper, for some warning times the collision energy required for an impulsive deviation technique can rise well above the theoretical catastrophic fragmentation limit. As a consequence the asteroid can fragment in an unpredictable number of pieces having different mass and velocity. The velocity associated to each piece of the asteroid uniquely determines its future trajectory.

In the paper, we consider two possible cases: the fragmentation being the desired outcome of the deviation strategy or the undesired product of a mitigation mission. In the latter case we will analyse the evolution of the cloud of fragments and the probability that the bigger pieces in the cloud has to impact the Earth. In the former case, we will investigate some possible strategies that allow us to minimize the risk of impact from the bigger pieces in the cloud.

Fragmentation is here considered as a stochastic process, using a different probability distribution to describe both fragment size and velocity distribution. The evolution in time of the cloud of fragments is computed by evoking Liouville's theorem for Hamiltonian systems and considering two body dynamics. The analysis of the dispersion of fragments and consequences of the fragmentation are applied to asteroid *Apophis* as illustrative example.

2. FRAGMENTATION OF ASTEROIDS

First, the asteroid resistance to fragmentation will need to be estimated in order to assess the likelihood of a fragmentation outcome from an impulsive mitigation technique. The critical specific energy Q^* is defined as the energy per unit of mass necessary to *barely catastrophically disrupt* an asteroid [3]; an asteroid is *barely catastrophically disrupted* when the mass of the largest fragment of the asteroid is half the mass of the original asteroid, or in other words, the remaining mass of the original asteroid is half the initial mass. If f_r is the fragmentation ratio, defined as:

$$f_r = \frac{m_{max}}{M_a}, \qquad (1.1)$$

where m_{max} is the mass of the largest fragment and M_a the initial mass of the asteroid, then a catastrophic fragmentation is defined as a fragmentation where $f_r < 0.5$.

This paper is addressing the issue of fragmentation of small to medium size asteroids. These are celestial objects ranging from 40m to 1km in diameter, which constitute the main bulk of the impact threat. Small objects in this range rely only on their material strength properties to avoid break up, while for large objects gravity plays a fundamental role. Asteroids smaller than 40m in diameter are expected to dissipate at a high altitude in the Earth atmosphere (2), thus nothing smaller than 40m will be included in this analysis. On the other hand, the survey of large objects, hence those above 1km diameter, is believed to be almost complete,

therefore only the remaining small not discovered asteroids pose a threat [10].

The uncertainty associated to the description of the fragmentation process is clear if one looks at the different scaling laws in the literature [11]. Furthermore, the exact value of Q^* depends on a number of factors, such as the composition and structure of the asteroid or the velocity and the size of the impactor. For the sake of the analysis in this paper, a complete and exact description of the fragmentation process is not required and an approximate estimate of the value of the critical specific energy Q^* is sufficient. The work of Ryan and Melosh [3] and Holsapple [12] provided the necessary tools to understand and approximate the qualitative limits of the critical specific energy Q^* for the range of studied asteroids. Fig. 1 shows the critical specific energy Q^* for asteroids ranging from 40m to 1km diameter, computed by using the scaling laws provided by Ryan and Melosh [3] and Holsapple [12].
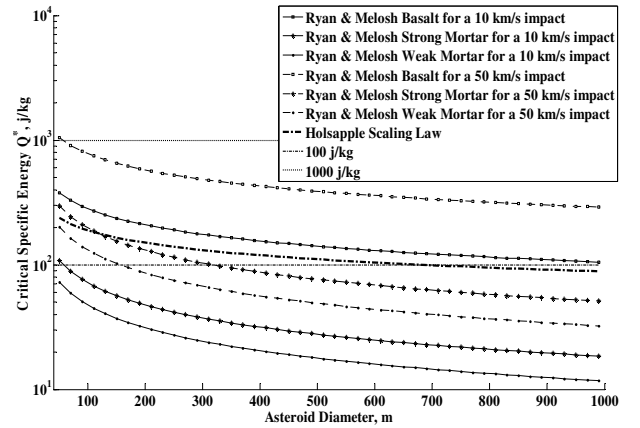
Fig. 1: Critical Specific Energy Q^* to barely catastrophically disrupt an asteroids with a diameter ranging from 40m to 1km using Ryan and Melosh [3] and Holsapple [12]. Ryan and Melosh [3] work provide a scaling law that takes into account both velocity of the impactor and impacted object diameter, while Holsapple [12]'s scaling law is only function of the impacted object diameter.

In the light of the results shown in Fig. 1, two general qualitative limits were considered: one at 1000 j/kg and a second at 100 j/kg. The 1000 j/kg limit can be interpreted as an almost certain catastrophic fragmentation, since the specific energy Q^* foreseen by the scaling laws in Fig. 1 is almost always below the 1000 j/kg limit, and even for some cases this limit is more than one order of magnitude above the predicted Q^*. Instead, the 100 j/kg is at the same energy level of most of the Critical Energies predicted by Fig. 1, and more importantly, the 100 j/kg limit is, in general, above the four predicted Q^* using Ryan and Melosh[3]'s Mortar strength. If asteroids have the tensile strength of "rubble piles", as the rotational state of small asteroids seems to indicate [13], the scaling laws for mortar tensile strength from Fig. 1 may be a good approximation. Hence, the 100 j/kg limit may be

2

considered as a reasonable fragmentation limit according the results of Ryan and Melosh [3] and Holsapple [12] scaling laws.

3. NEO DEFLECTION REQUIREMENTS

In order to compute the minimum deflection required to deviate a threatening asteroid, we will need to define the minimum distance that an asteroid needs to be shifted in order to miss the Earth. We consider one Earth radius $R_\oplus$ as the minimum required deviation distance and we take into account the gravitational pull of the Earth during the asteroid final close approach by using the following factor:

$$\varepsilon = \frac{r_a}{r_p} = \sqrt{1 + \frac{2\mu_e}{r_p v_\infty^2}} \qquad (2.1)$$

where r_a is the minimum distance between the hyperbola asymptote and the Earth, r_p is the perigee distance, which is $R_\oplus$ in our case, μ_e is the gravitational constant of the Earth and v_∞ the hyperbolic excess velocity. Note that the correcting factor will only depend on the hyperbolic excess velocity of the threatening object.

Table 1 summarizes the orbital characteristics of the test case that will be used in the subsequent analysis. *Apophis* is an interesting test case not only because is the most renowned asteroid among those posing a noticeable threat to Earth, but also because if another threat to Earth is to be appear, it will probably have orbital elements not too far from those of *Apophis* [14].

	Apophis
Semimajor axis *a*, km	0.922
Eccentricity *e*	0.191
Inclination *i*, deg	3.331
Ascending node Ω, deg	204.5
Pericenter angle ω, deg	126.4
Mean anomaly M, deg	222.3
Epoch, MJD	53800.5
t_{MOID}, MJD	62240.3
Hyperbolic factor ε	2.16
Impact velocity, km/s	12.62
Mass M_a, kg	2.7×10^{10} kg

Table 1: *Apophis* summary of orbital characteristics and mass. t_{MOID} stands for time at Minimum Orbital Interception Distance, and it is used here as equivalent to the time of the hypothetic impact.

3.1. Minimum Change of Velocity

Once the minimum distance to avoid collision is set, the minimum change of velocity to provide a safe deflection can be calculated. Fig. 2 presents the necessary change of velocity to deviate *Apophis* by a distance of $2.16 \times R_\oplus$ if the change is applied within an interval of time spanning 20 years before the hypothetical impact at time t_{MOID}. The minimum

change of velocity required to deviate an object by a given distance was computed by means of proximal motion equations expressed as a function of the variation of the orbital elements, the variation of the orbital elements was computed then with Gauss' planetary equations [15].
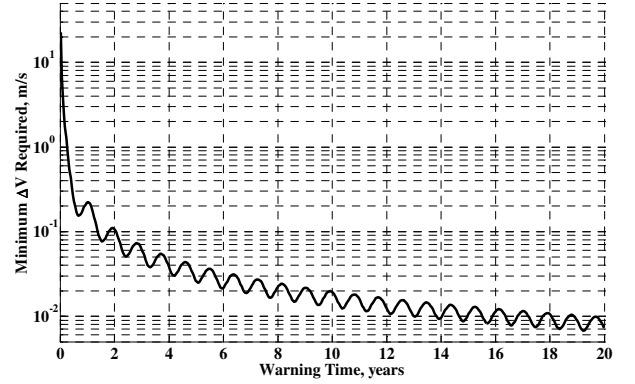
Fig. 2: Minimum Change of velocity to deviate *Apophis* by a distance $2.16 \times R_\oplus$ as a function of warning time. Warning time is referred here as the time available to correct the trajectory of a threatening object, thus the time difference between the instant at which the change of velocity takes place and the time of the hypothetic impact.

3.2. Kinetic Impactors and Nuclear Interceptors

Only impulsive mitigation actions could provide specific energies of the order of the Critical Energy Q* from Fig. 1. Hence, deflection strategies such as kinetic impactor and nuclear interceptor could possibly originate a catastrophic outcome as a result of a deviation attempt. The remaining of this section will briefly describe the main features of these two mitigations strategies, more comprehensive description can be found in other work by the authors [8].

The Kinetic Impactor is the simplest concept for asteroid hazard mitigation: the asteroid linear momentum is modified by ramming a mass into it. The impact is modelled as an inelastic collision resulting into a change in the velocity of the asteroid multiplied by a momentum enhancement factor [16]. This enhancement is due to the blast of material expelled during the impact, although if the asteroid undergoes a fragmentation process after the kinetic impactor has rammed into it, the enhancement factor should be considered 1. Accordingly, the variation of the velocity of the asteroid due to the impact is given by:

$$\Delta\mathbf{v}_a = \beta \frac{m_{s/c}}{(M_a + m_{s/c})} \Delta\mathbf{v}_{s/c}, \qquad (2.2)$$

where β is the momentum enhancement factor, $m_{s/c}$ is the mass of the kinetic impactor, M_a is the mass of the asteroid and $\Delta\mathbf{v}_{s/c}$ is the relative velocity of the spacecraft with respect to the asteroid at the time when the mitigation attempt takes place.

Knowing the minimum change of velocity required for a deflection (Fig. 2), Eq.(2.2) can be used to

3

compute the Specific Kinetic Energy (SKE) that an asteroid would have to absorb from a kinetic impactor attempting to modify the asteroid trajectory:

$$SKE = \frac{1}{2}\frac{m_{s/c}\Delta v_{s/c}^2}{M_a} = \frac{1}{2}\frac{\left(M_a + m_{s/c}\right)^2}{\beta^2 \cdot M_a \cdot m_{s/c}}\Delta v_a^2 \quad (2.3)$$

The Nuclear Interceptor strategy, instead, assumes a spacecraft carrying a nuclear warhead and intercepting with the asteroid. The model used in this study, fully described in *Sanchez et al.* [8], is based on a stand-off configuration over a spherical asteroid, i.e., the nuclear device detonates at a given distance from the asteroid surface. The energy released during a nuclear explosion is carried mainly by X-rays, neutrons and gamma radiation that are absorbed by the asteroid surface. This sudden irradiation of the asteroid, which causes material ablation and a large and sudden increase of the surface temperature, would induce a stress wave that while propagating through asteroid could trigger not only the surface material ablation that was intended to obtain a change of velocity, but also the fragmentation of the whole body. The Specific absorbed Nuclear Energy (SNE) is defined here as the portion of the energy release that is radiated over the asteroid divided by the mass of the asteroid.
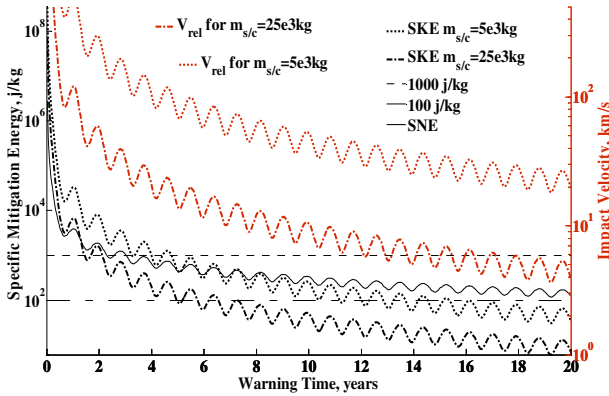
Fig. 3: Minimum specific kinetic energy (SKE) and specific absorbed nuclear energy (SNE) for a mitigation mission at a variable warning time (left Y axis). Relative impact velocities for two kinetic impactors (right Y axis), $m_{s/c}$=5000kg and $m_{s/c}$=25000kg. The enhancement factor is assumed 2 as a conservative value for this computation [8].

Fig. 3 presents the SKE and SNE as a function of warning time that kinetic impactor and nuclear interceptor, respectively, should provide given the delta-velocities required by Fig. 2. The two aforementioned fragmentation limits of 1000 j/kg and 100 j/kg are also superposed in the figure. The impact velocities for two possible impactors, ms/c=5000kg and ms/c=25000kg, are plotted as well with the right Y axis of Fig. 3. It should be noted that a Kinetic Impactor with ms/c=5000kg would need more than 100 km/s to deliver a collisional energy of 1000 j/kg or higher, which even taking into account retrograde impact trajectories does not seem possible with current technology. On the other hand, the two kinetic impactors used as example achieve energy values that

could possibly trigger a fragmentation with relative velocities lower than 50km/s, which can be achieve using retrograde orbits [17; 18].

The two suggested limits (1000 j/kg and 100 j/kg) must be taken cautiously when assessing the likelihood of fragmentation triggered by a nuclear interceptor. Since these two suggested limits were estimated from hypervelocity impact studies [19], the actual fragmentation energies for an asteroid being deflected by a nuclear device may be different, because of the different physical interaction. However, in this work we considered that the shock wave caused by an impact and the thermal stress wave generated by the nuclear explosion are analogous, and therefore the associated fragmentation energies are expected to have similar order of magnitude.

4. STATISTICAL MODEL OF A FRAGMENTED ASTEROID

As it can be concluded from the energetic requirements of a hazard mitigation mission, the risk of an undesired break-up of an asteroid during a deflection attempt cannot be ignored. The consequences of an undesired fragmentation can be evaluated by studying the evolution of the cloud of fragments generated during the break-up process. Instead of building a dynamical model of the fragmentation process, in this section we propose a statistical model of the initial distribution of the fragments with associated positions and velocities.

4.1. Fragmented Asteroid Dispersion

The position and velocity of every piece of a fragmented asteroid can be described as a stochastic process, even if the dynamical system is deterministic, since the initial conditions of the system are not known and they can only be assessed through a probability density function. Considering a scalar function describing the probability density of a dynamic system such as $\rho\left(\mathbf{X}(t)\right) = \rho(\mathbf{x}, \mathbf{v}; t)$, where $\rho(\mathbf{x}, \mathbf{v}; t)$ is the probability of a fragment to have position $\mathbf{x}$ and velocity $\mathbf{v}$ at a time t. The probability density function $\rho\left(\mathbf{X}(t)\right)$ relates to an initial probability density function $\rho\left(\mathbf{X}(0)\right)$ through:

$$\rho\left(\mathbf{X}(t)\right) = \int_\Gamma \delta\left(\mathbf{X}(t) - \phi^t(\mathbf{X}(0))\right)\rho\left(\mathbf{X}(0)\right)d\Xi\left(0\right) \quad (3.1)$$

where $\phi^t(\mathbf{X}(0))$ denotes the *flux* of the system, or evolution of the state $\mathbf{X}(0) = [\mathbf{x}(0), \mathbf{v}(0)]^T$ over a time-span t so that $\phi^t(\mathbf{X}(0)) = [\mathbf{x}(t), \mathbf{v}(t)]^T$, $\delta(\mathbf{y})$ is a multi-dimensional Dirac-delta, which represents the product of the one-dimensional Dirac-delta functions, that will allow a probability $\rho\left(\mathbf{X}(0)\right)$ to be added to the total probability of $\rho\left(\mathbf{X}(t)\right)$, only if the initial state vector $\mathbf{X}(0)$ can effectively evolve to $\mathbf{X}(t)$, and finally, $d\Xi\left(0\right)$ refers to the product of the one-dimensional differentials components of the vector $\mathbf{X}(0)$, i.e.,

$dx \cdot dy \cdot dz \cdot dv_x \cdot dv_y \cdot dv_z$, and defines the volume of an infinitesimal portion of the phase space Γ, which is the feasible phase space where the system evolves.

If we introduce the new variable $\mathbf{z} = \phi^t(\mathbf{X}(0))$ and the associated Jacobian determinant as $|\mathbf{J}| = \left| \dfrac{\partial \phi^t(\mathbf{X}(0))}{\partial \mathbf{X}(0)} \right|$, we can substitute the differential $d\Xi(0)$ by $d\zeta/\|\mathbf{J}\|$ in Eq.(3.1), where $d\zeta$ is the product of the one-dimensional differentials components of the vector $\mathbf{z}$ and $\|\mathbf{J}\|$ is the absolute value of the Jacobian determinant. This allows us to integrate using the phase space at time t and Eq.(3.1) results in the following integration:

$$\rho\big(\mathbf{X}(t)\big) = \int_\Gamma \delta\big(\mathbf{X}(t) - \mathbf{z}\big)\rho\big(\phi^{-t}(\mathbf{z});0\big)\frac{d\zeta}{\|\mathbf{J}\|} \qquad (3.2)$$

From the Liouville's theorem, which states that for a Hamiltonian system the density of states in the phase space remains constant with time [20], we know that $\|\mathbf{J}\| = 1$, thus Eq.(3.2) can be solved giving:

$$\rho\big(\mathbf{X}(t)\big) = \rho(\phi^{-t}(\mathbf{x}, \mathbf{v});0) \qquad (3.3)$$

Eq. (3.3) implies that the probability that a particular fragment has position $\mathbf{x}$ and velocity $\mathbf{v}$ at a time t is the same probability of having the initial conditions that can make the fragment dynamically evolve to the particular state $\mathbf{X}(t)$.

If we now compute the state transition matrix $\mathbf{\Phi}(t,t_0)$:

$$\mathbf{\Phi}(t,t_0) = \begin{bmatrix} \dfrac{\partial \mathbf{x}(t)}{\partial \mathbf{x}(t_0)} & \dfrac{\partial \mathbf{x}(t)}{\partial \mathbf{v}(t_0)} \\[2mm] \dfrac{\partial \mathbf{v}(t)}{\partial \mathbf{x}(t_0)} & \dfrac{\partial \mathbf{v}(t)}{\partial \mathbf{v}(t_0)} \end{bmatrix}, \qquad (3.4)$$

we can directly map the initial state vector $\mathbf{X}(t_0)$ to the final state vector $\mathbf{X}(t)$, which is necessary to calculate Eq.(3.3):

$$\begin{bmatrix} \mathbf{x}(t) \\ \mathbf{v}(t) \end{bmatrix} = \mathbf{\Phi}(t,t_0)\begin{bmatrix} \mathbf{x}(t_0) \\ \mathbf{v}(t_0) \end{bmatrix} \qquad (3.5)$$

Since we are interested in studying the dispersion of a cloud of particles, we can work in relative coordinates to study the differences in position and velocity with respect the unperturbed orbit of the asteroid prior to fragmentation. Eq.(3.5) can be simplified by assuming that all the fragmented particles depart from the centre of mass of the asteroid (i.e., the relative initial position $\Delta\mathbf{x}(t_0)$ is 0), and by computing only the relative final position $\Delta\mathbf{x}(t)$:

$$\mathbf{x}(t) = \frac{\partial \mathbf{x}(t)}{\partial \mathbf{v}(t_0)}\mathbf{v}(t_0) \qquad (3.6)$$

This simplifies the problem considerably since only the 3×3 transition matrix $\partial\mathbf{x}(t)/\partial\mathbf{v}(t_0)$ is required. The transition matrix is given by the product of the linear proximal motion equations and the Gauss' planetary equations (for further details see Vasile and Colombo [15]). This calculation provides a linear approximation of the nonlinear two body dynamics, but if the dispersive velocity is small compared to the nominal velocity of the unfragmented asteroid, it is a workable approximation [15].

Since we are interested in the probability to find a fragment in a certain position in space at a particular time t, the probability function $\rho(\mathbf{x},\mathbf{v};t)$ will need to be integrated over all the feasible space of velocities:

$$P(\mathbf{x};t) = \int_\Gamma \rho(\mathbf{x},\mathbf{v};t)d\upsilon(t) = \int_\Gamma \rho(\phi^{-t}(\mathbf{x},\mathbf{v});0)d\upsilon(t) \quad (3.7)$$

where $d\upsilon(t)$ is the product of the one-dimensional differentials components of the velocity, $dv_x \cdot dv_y \cdot dv_z$.

Since the probability density function $\rho(\mathbf{x},\mathbf{v};0)$ is the probability to have a fragment in a position $\mathbf{x}(0)$ with velocity $\mathbf{v}(0)$ and we already assumed that the dispersion of fragments initiates from the centre of mass of the unfragmented asteroid, then we can express $\rho(\mathbf{x},\mathbf{v};0)$ as the product of two separated probability density function:

$$\rho(\mathbf{x},\mathbf{v};0) = \delta(\mathbf{x}(0)-\mathbf{r_0}) \cdot G(\mathbf{v}(0)) \qquad (3.8)$$

where $\delta(\mathbf{x}(0)-\mathbf{r_0})$ is giving the probability of a particular fragment to have position $\mathbf{x}(0)-\mathbf{r_0}$, where $\mathbf{r_0}$ is the position of the centre of mass of the unfragmented asteroid at $t = 0$, and $G(\mathbf{v}(0))$ is associating the probability to have velocity $\mathbf{v}(0)$ to the same fragment. Now, Eq.(3.7) can be rewritten using Eq.(3.8) as:

$$P(\mathbf{x};t) = \int_\Gamma \delta(\phi^{-t}(\mathbf{x},\mathbf{v})_\mathbf{x} - \mathbf{r_0}) \cdot G(\phi^{-t}(\mathbf{x},\mathbf{v})_\mathbf{v})d\upsilon(t) \; (3.9)$$

where $\phi^{-t}(\mathbf{x},\mathbf{v})_\mathbf{x}$ and $\phi^{-t}(\mathbf{x},\mathbf{v})_\mathbf{v}$ are the components of the position and velocity respectively of the *flux* $\phi^{-t}(\mathbf{x},\mathbf{v})$. Now, similar to what it was done with Eq.(3.1), the element of volume of the space of velocities $d\upsilon(t)$ can be related to the element $d\xi(0) = dx \cdot dy \cdot dz$ through their Jacobian:

$$d\upsilon(t) = \left\|\frac{\partial \mathbf{v}(t)}{\partial \mathbf{x}(0)}\right\| d\xi(0) \qquad (3.10)$$

allowing us to solve the integral in Eq.(3.7):

$$P(\mathbf{x};t) = \left\|\frac{\partial \mathbf{v}(t)}{\partial \mathbf{x}(0)}\right\| G((\phi^{-t}(\mathbf{x},\mathbf{v_*})_\mathbf{v}) \qquad (3.11)$$

where $\mathbf{v_*}$ is the solution of the equation:

$$\phi^{-t}(\mathbf{x},\mathbf{v_*})_\mathbf{x} = \mathbf{r_0} \qquad (3.12)$$

so that the $\delta(\phi^{-t}(\mathbf{x},\mathbf{v})_\mathbf{x} - \mathbf{r_0})$ is 1. Besides, the absolute value of the Jacobian in Eq.(3.11) relates to the transition Matrix $[\partial\mathbf{x}(t)/\partial\mathbf{v}(t_0)]$ in Eq.(3.6) as follows:

$$\left\|\frac{\partial \mathbf{v}(t)}{\partial \mathbf{x}(0)}\right\| = \frac{1}{\left\|\dfrac{\partial \mathbf{x}(0)}{\partial \mathbf{v}(t)}\right\|} = \frac{1}{\left\|\dfrac{\partial \mathbf{x}(t)}{\partial \mathbf{v}(t_0)}\right\|} \qquad (3.13)$$

Finally, the probability to find a piece of asteroid in a particular position at a given time after a fragmentation is given by:

$$P(\mathbf{x};t) = \frac{1}{\left\| \dfrac{\partial \mathbf{x}(t_0)}{\partial \mathbf{v}(t)} \right\|} G\left(\left[\frac{\partial \mathbf{x}(t)}{\partial \mathbf{v}(t_0)} \right]^{-1} \mathbf{x}(t) \right) \quad (3.14)$$

4.2. Velocity Dispersion Model

We have assumed, in Eq.(3.8), that the probability density function depends on two terms, a Dirac delta such as $\delta(\mathbf{x}(0) - \mathbf{r_0})$ for the position, which is equivalent to one Dirac delta function for each one of the components of the vector $\mathbf{x}(0)$, and a function $G(\mathbf{v}(0))$ that describes the dispersion of the values of the initial velocity $\mathbf{v}(0)$. For the latter purpose, we will use three Gaussian distribution; each Gaussian distribution will describe the velocity dispersion in one direction of the Hill's reference frame $\hat{t} - \hat{n} - \hat{h}$ (or tangential, normal and out-of-plane direction):

$$G\left(v_t(0), v_n(0), v_h(0)\right) = \frac{1}{\sigma_t\sqrt{2\pi}} e^{\frac{-(v_t - \mu_t)^2}{2\sigma_t^2}}$$
$$\cdot \frac{1}{\sigma_n\sqrt{2\pi}} e^{\frac{-(v_n - \mu_n)^2}{2\sigma_n^2}} \cdot \frac{1}{\sigma_h\sqrt{2\pi}} e^{\frac{-(v_h - \mu_h)^2}{2\sigma_h^2}} \quad (3.15)$$

Six parameters will be needed in order to define the dispersion of velocities: three mean velocities $\boldsymbol{\mu} = [\mu_t \quad \mu_n \quad \mu_h]$, and three standard deviations $\boldsymbol{\sigma} = [\sigma_t \quad \sigma_n \quad \sigma_h]$.

Assuming a kinetic impactor scenario, we can think that, at an infinitesimal instant after the impact, but before the fragmentation takes place, the system asteroid-spacecraft form a single object, which moves according to the law of conservation of linear momentum. In fact, after the kinetic impactor mission triggers a catastrophic fragmentation, it is reasonable to think that the system asteroid-spacecraft would preserve the total linear momentum. Hence, given the SKE of a particular collision, Eq.(2.3) will provide the change of velocity of the centre of mass of the system only by considering the momentum enhancement factor β equal 1. It seems also sensible to think of the mean vector $\boldsymbol{\mu} = [\mu_t \quad \mu_n \quad \mu_h]$ as the change of velocity of the centre of mass, since the highest probability to find a fragment should be at the centre of mass of the system. As a result, the norm of the mean of the dispersion should be:

$$|\boldsymbol{\mu}| = |\Delta \mathbf{v_a}| = \frac{\sqrt{2 M_a m_{s/c} SKE}}{(M_a + m_{s/c})} \quad (3.16)$$

The direction of $|\boldsymbol{\mu}|$ is defined by the direction of the vector $\Delta \mathbf{v}_{s/c}$. Since the trajectory of kinetic impactor should be designed to achieve the maximum possible deviation, $|\boldsymbol{\mu}|$ should be directed along the tangential direction [15]. Accordingly, given the SKE of the collision, the mean velocity dispersion vector can be taken as:

$$\boldsymbol{\mu} = \left[\frac{\sqrt{2 M_a m_{s/c} SKE}}{(M_a + m_{s/c})} \quad 0 \quad 0 \right] \quad (3.17)$$

Just as it is sensible to think that after a dish has shattered on the floor, the smallest fragments are always found the furthest, one would expect that the smaller the fragments of the asteroid are the larger will be their velocity dispersion $\boldsymbol{\sigma} = [\sigma_t \quad \sigma_n \quad \sigma_h]$, hence the mass of the fragment must have an influence on the dispersion of velocities. Let us assume that a fragment with mass m_i has a velocity Δv_i defined by an inelastic collision such that (note that in the following, it is considered that $m_{s/c}$ is always orders of magnitude smaller than both M_a and m_i, thus $M_a + m_{s/c} \approx M_a$ and $m_i + m_{s/c} \approx m_i$):

$$m_i \Delta v_i \approx m_{s/c} \Delta v_{SKE \cdot m_i} \quad (3.18)$$

where $\Delta v_{SKE \cdot m_i}$ is a collisional velocity such that the fragment m_i takes with it its share of collisional energy SKE, that is:

$$\Delta v_{SKE \cdot m_i} = \sqrt{\frac{2 \cdot SKE \cdot m_i}{m_{s/c}}} \quad (3.19)$$

Clearly, $\Delta v_{SKE \cdot m_i}$ is only a mathematical entity that helps us to develop the hypothesis at hand, the real impact occurs between the unfragmented asteroid with mass M_a and the spacecraft with mass $m_{s/c}$ at a relative velocity of:

$$\Delta v_{s/c} = \sqrt{(2 \cdot SKE \cdot M_a)/m_{s/c}} \quad (3.20)$$

Writing Eq.(3.19) as a function of the *real* impact velocity $\Delta v_{s/c}$ of the spacecraft, Eq.(3.20), leads us to:

$$\Delta v_{SKE \cdot m_i} = \sqrt{\frac{m_i}{M_a}} \cdot \Delta v_{s/c} \quad (3.21)$$

Using the virtual inelastic collision Eq.(3.18) and Eq.(3.21), we can write Δv_i as:

$$\Delta v_i = \frac{m_{s/c}}{m_i} \sqrt{\frac{m_i}{M_a}} \cdot \Delta v_{s/c} \quad (3.22)$$

As it has been said before, the centre of mass of the cloud of fragments is likely to follow the law of conservation of linear momentum (i.e., $M_a \Delta v_a \approx m_{s/c} \Delta v_{s/c}$), hence Eq.(3.22) finally settles down to the following expression:

$$\Delta v_i = \sqrt{\frac{M_a}{m_i}} \cdot \Delta v_a \quad (3.23)$$

Note that Eq.(3.23) is only one step away from:

$$\frac{1}{2} m \Delta v^x = constant \quad (3.24)$$

when x is equal to 2. Hence, we are assuming a homogenous distribution of the translational kinetic energy among all the fragments, or equipartition of translational kinetic energy. Several experimental works have intended to adjust a similar relation (i.e.,

6

Eq.(3.24)) to their fragment size and velocity experimental data; Gault *et al.* [21] found an exponent of 2.25 for his cratering experiments, while Davis and Ryan [19] found exponents between 1.92 and 1.41 on their fragmentation experiments. An equipartition effect was also suggested by Wiesel [22] while studying the explosion of objects such as spacecrafts in Earth orbit.

Recalling the definition of standard deviation, $\sigma = \sqrt{\langle \Delta \mathbf{v}^2 \rangle - \langle \Delta \mathbf{v} \rangle^2}$, and assuming $\langle \Delta \mathbf{v} \rangle = 0$ for a homogeneous spherical dispersion from the centre of mass of the cloud of fragments, we can compute the norm of the standard deviation of the velocities $\sigma(m_i)$ using Eq.(3.23) as:

$$\sigma(m_i) = \sqrt{\frac{M_a}{m_i}} \cdot \sigma_0 \qquad (3.25)$$

where σ_0 is now:

$$\sigma_0 = \frac{\Delta v_a}{k} \qquad (3.26)$$

with k a constant value. The constant k is 1 if we consider the velocity of the fragment with mass m_i as described above, i.e., Eq.(3.23).

In fact, one could think of k as the efficiency of transmission of the collisional energy. If part of the collisional energy is lost in processes such as melting or breaking, one could expect k to be larger than 1, on the other hand, k could also be smaller than 1 for fragments coming from areas in the asteroid where there was higher reservoir of collisional energy, e.g., close to the impact site. Therefore, it would be sensible to expect that small fragments may have k equal to 1 or smaller, since small fragments must come from areas with a higher reservoir of collisional energy so that this energy was able to break the material to smaller pieces. Large fragments may have instead k larger than 1 from opposite reasons. Using the experimental data published by Davis and Ryan [19], one can fit their experiments with velocity dispersion data available to find an average value of k. Doing so, k results 1.4. Thus,

$$\sigma_0 = \frac{\Delta v_a}{1.4} \qquad (3.27)$$

To finish, the norm of standard deviation of velocity is $\sigma(m_i)$ as in the Eq.(3.25), and since we assume an homogeneous spherical dispersion on the initial velocities at the break-up point, we can write the vector of the standard deviation as assuming three equal 1-dimensional values:

$$\boldsymbol{\sigma} = \left[\frac{1}{\sqrt{3}} \sqrt{\frac{M_a}{m_i}} \cdot \sigma_0 \quad \frac{1}{\sqrt{3}} \sqrt{\frac{M_a}{m_i}} \cdot \sigma_0 \quad \frac{1}{\sqrt{3}} \sqrt{\frac{M_a}{m_i}} \cdot \sigma_0 \right] (3.28)$$

5. <u>EVOLUTION OF THE CLOUD OF</u>

<u>FRAGMENTS</u>

The following six figures, Fig. 4 to Fig. 9, show the evolution of the probability density function of a fragmentation occurring after providing 500 j/kg of

collisional energy to *Apophis* (test case in Table 1). Such a kinetic impact would provide an approximate change of velocity of $\Delta v_a = 0.02\, m/s$ by using an impactor with mass $m_{s/c}$ of 10,000kg. The figures are showing the volume enclosing 97% chances to find each single 10^{10}kg-fragment at different times or different true angles. Break-up is set to occur at the pericentre of the unperturbed orbit, and the sequence of figures show the 97% volume at true anomalies of 45^0, 90^0, 180^0, 270^0, 315^0 and 360^0.
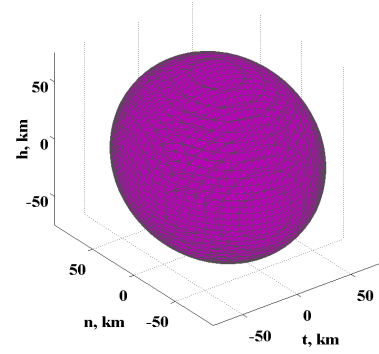
Fig. 4: ~ 97% probability volume for a fragment with mass 10^{10}kg at true anomaly of 45^0.
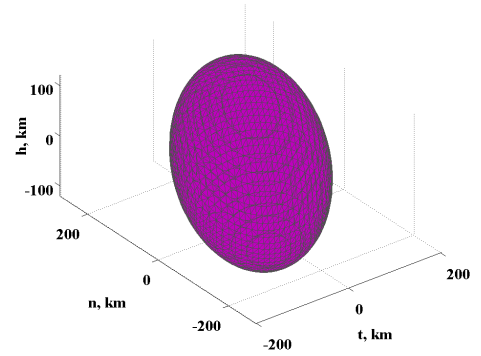
Fig. 5: ~ 97% probability volume for a fragment with mass 10^{10}kg at true anomaly of 90^0.
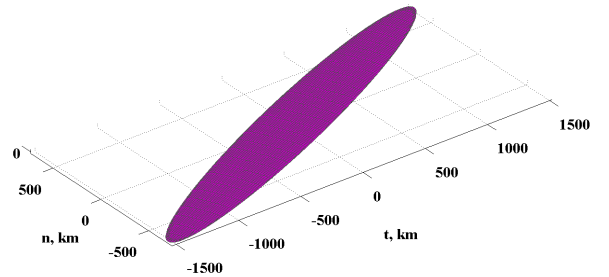
Fig. 6: ~ 97% probability volume for a fragment with mass 10^{10}kg at true anomaly of 180^0.

7
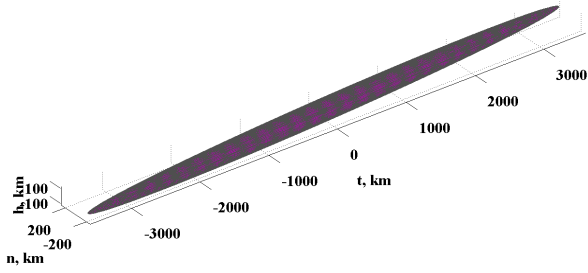
Fig. 7: ~ 97% probability volume for a fragment with mass 10^{10}kg at true anomaly of 270^0.
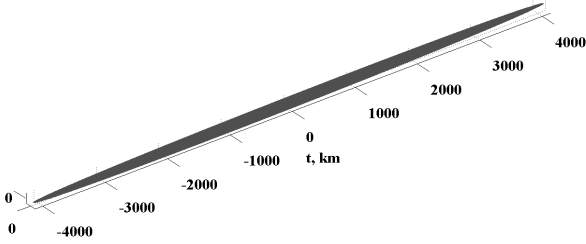
Fig. 8: ~ 97% probability volume for a fragment with mass 10^{10}kg at true anomaly of 315^0.
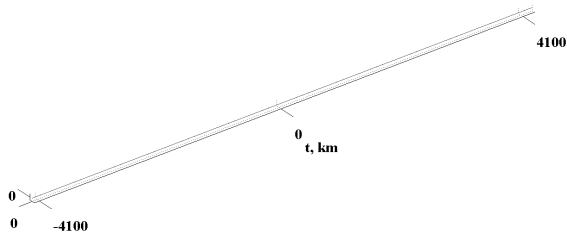
Fig. 9: ~ 97% probability volume for a fragment with mass 10^{10}kg at true anomaly of 360^0.

The volumes plotted in Fig. 4 to Fig. 9 can be also understood as the physical shape of the cloud of fragments of a certain size, since the probability density function is describing the regions where, statistically at least, there is a higher density of particles. The most prominent feature that stands out from the images above is the ellipsoidal shape of volume enclosing a particular probability, or cloud of particles. In order to better understand the dynamics of the dispersive cloud of particles, we can try to understand the evolution of the four salient features of the elliptical cloud. These four features are: the semimajor axis a, the semiminor axis b, the dispersion along the h axis or out-of-plane and the angle α between the semimajor axis a and the tangential direction axis t.
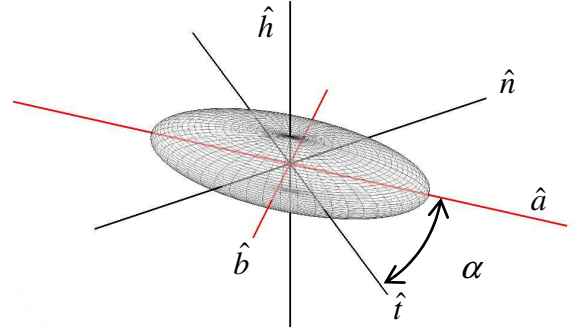
Fig. 10: schematic of the 4 features describing the shape and attitude of the elliptic shaped cloud of fragments.

Fig. 11 summarizes the evolution of the four aforementioned features that describe the volume enclosing 97% probability to find each one of the existing fragments with mass of 10^{10}kg. Larger fragments will have smaller volumes, but the same shape, since their velocity dispersion σ will be smaller by a factor of $\sqrt{10^{10}kg / m_{>1\times10^{10}kg}}$, while the opposite occurs for smaller objects. Fig. 11 extents also the evolution shown in Fig. 4 to Fig. 9 to complete a two years propagation from the break-up point.
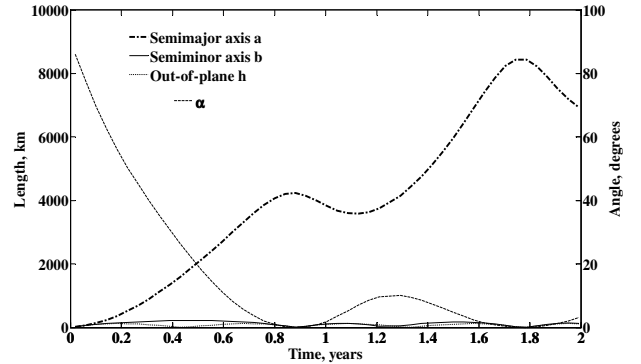
Fig. 11: Two years evolution of the four salient features defining the elliptical cloud enclosing 97% probability to find each fragment of 10^{10}kg.

It is important to note that the evolution of the shape of the cloud is essentially driven by the dynamics of the system, thus the proximal motion equations that we used to define the transition matrix in Eq.(3.6). For example, among the three parameters defining the size of the ellipse, the semimajor axis a is the only parameter that is unbounded, much like the change of velocity in tangential direction, which causes an unbounded drift from the unperturbed initial orbit.

6. **CONSEQUENCES OF A FRAGMENTATION**

If the impact with *Apophis* is assumed to occur at the MOID point, then, the impact likelihood can be calculated by integrating over the volume inside a sphere centred at the *Apophis*' MOID point with radius equal to the Earth capture volume $dV(r)$:

8

$$L = \int_{V(r=0)}^{V(r=\varepsilon \cdot R_{\oplus})} P(\mathbf{x};(t_{MOID}-t_0)) \cdot dV(r) \qquad (5.1)$$

Note that the capture volume is approximated by the Earth radius corrected with the aforementioned hyperbolic factor ε, to account for the gravitational focusing of the Earth.

From Eq.(5.1) we can see that the total impact likelihood for a particular fragment size is only a function of the time of the closest approach t_{MOID} (see Table 1), the time at which the break up occurred (the difference between these two times is here referred to as the warning time) and the specific collisional energy used to break up the asteroid. Fig. 12 shows the evolution along warning time of the impact likelihood for 10^{10}kg-fragments emanating from a hypothetical fragmentation of *Apophis*.
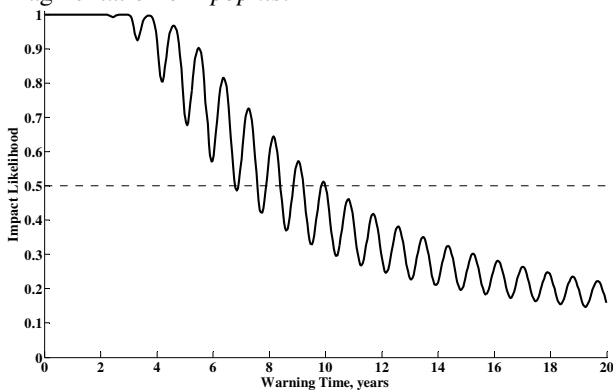
Fig. 12: Impact likelihood for *Apophis*'s 10^{10}kg-fragments as a function of warning time or time span between break-up and impact. The integrated volume is a sphere of radius $2.16R_{\oplus}$ with centre at the position of the unperturbed *Apophis* (Table 1) at time t_{MOID}. Break up is triggered by an $m_{s/c}$ of 10,000kg providing 500 j/kg of SKE, which in turn provides a mean velocity $\boldsymbol{\mu} \sim [0.02m/s \quad 0 \quad 0]$ and a standard deviation $\boldsymbol{\sigma} \sim [0.013 \quad 0.013 \quad 0.013] m/s$ to the 10^{10}kg-fragments.

An important difference of the calculation in Fig. 12 with respect the calculations in Fig. 4 to Fig. 9 is the fact that for Fig. 12 the break up of the asteroid is moving backwards in time, in order to have an increase in warning time, while the hypothetical impact time t_{MOID} is kept fixed. A consequence of this is that the break up occurs at different orbital positions of the unperturbed orbit of *Apophis*, and the periodic variations of the impact likelihood that can be observed in Fig. 12 are in fact due to this change of the orbital position of the break up point. The periodic minimum occurs at each orbit when the break up is at the pericentre of the orbit, and the maximum occurs at the apocentre. This is not surprising, since, for a fixed change of velocity δv of a fragment, the maximum change of orbital period occurs when the orbital velocity is maximum, which happens at the pericentre, therefore the maximum dispersion of fragments

happens also when the break up point is at the pericentre.

6.1. Fragment size distribution

It is out of the scope of this paper to describe the physics of the fragmentation of a brittle solid, such as an asteroid, and a simple statistical distribution of fragments will serve better to our purposes, which are to discern the intrinsic risks of the asteroid hazard mitigation.

Early works in collisional fragmentation already used accumulative power law distribution to model fragment size distribution [23]. Two- or three-segments power laws had been found to fit much better to experimental data [19; 24], specially when the fragmentation data comprises sizes many orders of magnitude smaller than the original size. However, for the analysis carried out here we will use only one segment accumulative power law distribution such as:

$$N(> m) = Cm^{-b} \qquad (5.2)$$

since this is already an acceptable approximation for a qualitative analysis of a range of 3 orders of magnitude in mass. In Eq.(5.2), if m_{max} is the mass of the largest fragment, $N(\geq m_{max})$ must be 1, therefore the constant C must be:

$$C = m_{max}^{b} \qquad (5.3)$$

Now, If we integrate the mass over all the particles, the total mass must be equal to the unfragmented asteroid mass M_a:

$$M_a = \int_{M_{max}}^{0} m \cdot dN = \left[\frac{bC}{(1-b)} \right] m_{max}^{1-b} \qquad (5.4)$$

Using Eq.(5.3) in Eq.(5.4), the exponent b becomes a function only of the ratio between the largest fragment mass m_{max} and the total mass of the asteroid M_a:

$$b = \left(1 + \frac{m_{max}}{M_a} \right)^{-1} \qquad (5.5)$$

where the fraction m_{max}/M_a is *fragmentation ratio* f_r.

Fig. 13 shows the number of fragments of different sizes expected for three catastrophic fragmentations using a power law distribution such as Eq.(5.2): $f_r = 0.5$ (blue bars), $f_r = 0.25$ (green bars) and $f_r = 0.1$ (red bars). Only the range of fragments that can pose threat to Earth are shown in the figure. It is interesting to note that the higher the level of disruption the lesser the number of dangerous fragments.
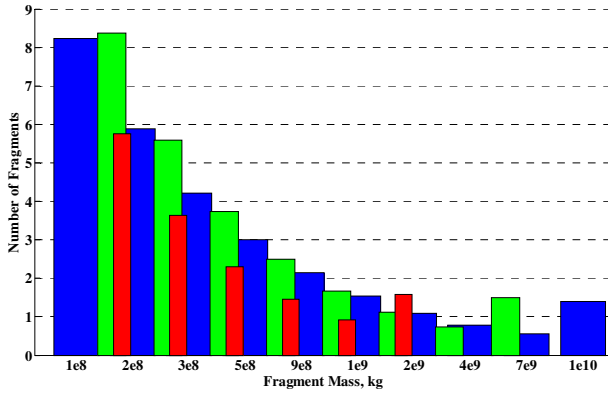
Fig. 13: Approximated number of pieces expected to be found in a fragmentation cloud of an asteroid with $2.7x10^{10}$kg of mass resulting from disruptions with f_r=0.5 (blue bars), f_r=0.25 (green bars) and f_r=0.1 (red bars). The largest fragment, i.e., surviving mass of the asteroid, is counted in the initial bin of the histogram for each level of disruption.

6.2. Average Predicted Impacts

Here we present the impact likelihood over a time span of 20 years. Five different size samples were computed: 10^{10}kg, 10^9kg, $5x10^9$kg,, 10^8kg and $5x10^8$kg. By definition, from a fragmentation with f_r=0.5, we have at least a large fragment with half the mass of the original asteroid, $1.35x10^{10}$kg, the remaining pieces of the asteroid are assumed to follow the power law distribution such as Eq.(5.2), and their impact likelihoods approximated to the closest of the calculated masses. Table 2 summarizes the computed fragment groups and the average number of fragments belonging to each group.

Bins	N(f_r=0.5)	Mass
$1.35x10^{10} \, kg \geq m > 7x10^9 \, kg$	2	$1x10^{10} \, kg$
$7x10^9 \, kg \geq m > 2x10^9 \, kg$	2	$5x10^9 \, kg$
$2x10^9 \, kg \geq m > 7x10^8 \, kg$	4	$1x10^9 \, kg$
$7x10^8 \, kg \geq m > 2x10^8 \, kg$	8	$5x10^8 \, kg$
$2x10^8 \, kg \geq m > 9x10^7 \, kg$	13	$1x10^8 \, kg$

Table 2: Fragment groups used for the computation of impact likelihood and average number of impacts for a barely catastrophic fragmentation. Note that the smallest mass is $9x10^7$kg, since the lower limit is set by the lower diameter limit of 40m.
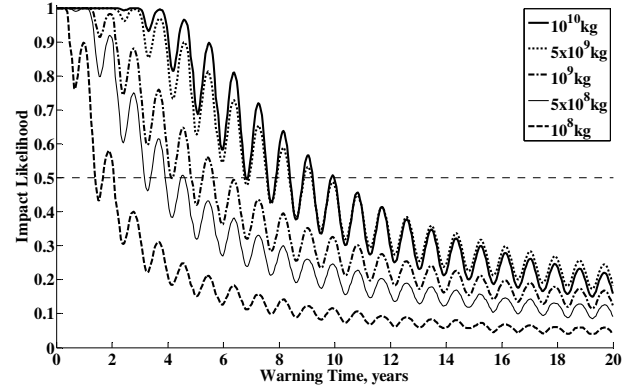
Fig. 14: Impact likelihood evolutions of the 5 fragments size computed.
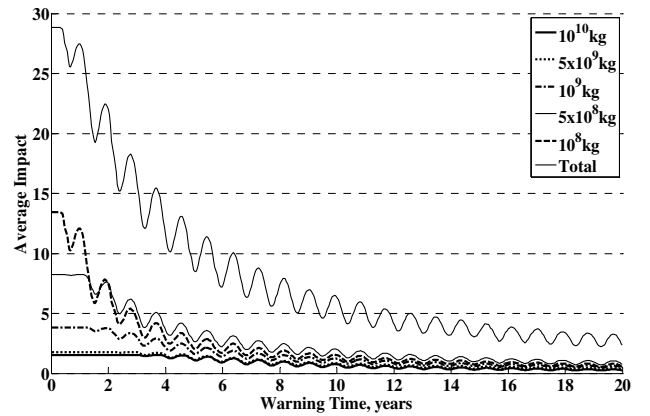
Fig. 15: Average number of impacts for each fragment size group.

Fig. 14 and Fig. 15 show the evolution with warning time of the individual impact likelihood for each fragment size and the number of impacts that should be expected for each fragment size, which is simply the result of the number of fragments multiplied by the impact likelihood. As was expected, the smaller a fragment is the lower its impact likelihood, which is due to the higher velocity dispersion. Despite that, the number of expected impacts grows with a decreasing mass of the fragments and even if the break-up occurred 20 years in advance still a few impacts should be expected.

6.3. Expected Damage

As shown in Fig. 15 from last section, if an asteroid hazard mitigation causes the break-up of an asteroid such as *Apophis*, several impacts of small fragments could be expected even if the fragmentation or break-up occurred 20 years prior to the forecasted impact. Nevertheless, the number of expected impacts is not a good figure to evaluate the risk that these small objects spawn to Earth, therefore the work of Hills and Goda [25] and Chesley and Ward [26] will be used to assess the damage that these smaller fragments can cause and, finally, the damage will be compared with the initial damage that the unshattered *Apophis* could have caused.

10

Obviously an asteroid or fragment threatening to impact with the Earth would have 2/3 chances to fall into the water and only 1/3 to fall into land. A small land impact trends to be much more localized than a sea impact, since water can transmit the impact energy very large distances on two-dimensional waves. Adding to the efficient energy propagation, the high coastal density population makes water impacts a major element of the impact hazard.

Table 3 shows the expected damage for both the unshattered *Apophis* and each one of the fragment sizes analysed earlier. Land damage is assessed using Hills and Goda [25]'s calculations; for all fragments size, the radius of destruction is taken from the worse case between soft and hard stone of a 20km/s impact. Water damage, instead, is evaluated using data accounting also for 20km/s water impacts found in Stokes *et al* [10]., which were computed using the assessment on damage generated by tsunamis from Chesley and Ward [26]. Since *Apophis*' impact velocity is only 12.62km/s (Table 1), the predicted areas were scaled by the collisional energy fraction to the power of 2/3, which is believed to be how the explosive devastation area scales with the energy [27].

Mass	Diameter	Land [km^2]	Water [km^2]	Weighted [km^2]
2.7x10^{10}kg	270m	~5,920	~57,000	~40,000
1x10^{10}kg	194m	~4,080	~25,000	~17,700
5x10^{9}kg	154m	~3,140	~10,000	~7,600
1x10^{9}kg	90m	~2,080	~250	~860
5x10^{8}kg	71m	~750	~40	~280
1x10^{8}kg	41m	~42	~0	~14

Table 3: Expected damaged area caused by the unshattered asteroid and its fragments. The weighted damage estimation is calculated using a 2/3 and 1/3 weights for water and land impacts respectively.

Table 3 also includes a *weighted* damaged ratio. The weighted damaged ratio considers the mean damage of a statistical distribution of impacts. One could think that although for small fragments the number of impacts is high enough to make the weighted damage a good approximation, for the largest fragments and especially for the unfragmented asteroid the approximation can drive to misleading results, since a single fragment would not cause a *weighted* damage, but one of the two options, i.e., either land or water impact. Only by the data in Table 3, the most worrying scenario would be if the unshattered *Apophis* was meant to impact land, and because of a failed attempt to mitigate the threat, at least 1 of the fragments with mass 5x10^{9}kg or larger, possibly up to 4 objects of those sizes, fall into the water, which has 33% probability to happen if we consider the fall of each fragment as statistically independent. On the other hand, if *Apophis* is meant to hit the sea, only the case that all the large fragments fall into the water would increase the initial unfragmented damage. To sum up, there is only 35% probability to increase the damage by fragmentation of the original asteroid, if both the

unshattered object and all its fragments fall into Earth. Highlighting the latter result, the weighted damage is used on the rest of the analysis of consequences of a fragmentation.

Fig. 16 shows the total damage ratio of the fragmented *Apophis*, together with the ratio of the unshattered object. The damage ratio of the fragmented case is computed by adding up the predicted weighted damage of each size, thus multiplying Table 3 damaged areas by results in Fig. 15, and then dividing the total area by the weighted damaged area of the unfragmented *Apophis*, ~40,000km^2. We shall remind that in this example the fragmentation was triggered by a kinetic impactor with a $m_{s/c}$ of 10,000kg providing 500 j/kg of SKE. If *Apophis* would not shatter under such a collisional energy the asteroid would be deflected with a velocity of $\mu \sim [0.02m/s \quad 0 \quad 0]$, considering an enhancement factor β of 1. With this change in velocity, *Apophis* would miss the Earth when the minimum required change in velocity is smaller than 0.02 m/s, which occurs between 7 and 10 years (see Fig. 2). Fig. 16 shows the damage ratio of the unshattered object, which has been computed by considering the change of velocity $\mu \sim [0.02m/s \quad 0 \quad 0]$ with an added 25% error in both direction and modulus of μ to account for uncertainties during the mitigation mission, without this hypothetical error in the kinetic impactor performance, the damaged ratio would simply resembles a step function.
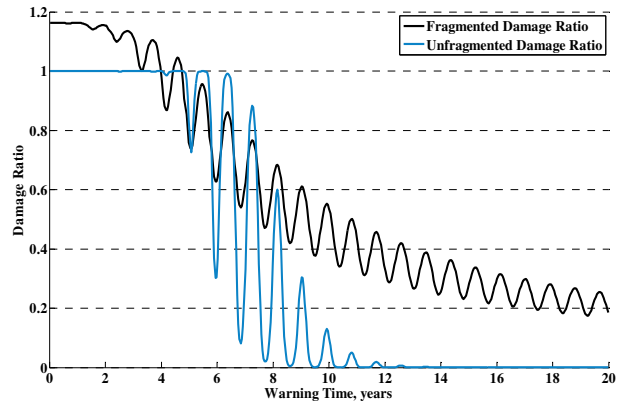
Fig. 16: Damage ratios of *Apophis*: fragmented case (black line) and unfragmented case (blue line) with 25% error in the delta-velocity.

Fig. 16 demonstrates that if the outcome of a deflection mission is a barely catastrophic disruption (f_r=0.5), then there is a high probability to increase the damage to the Earth, even for very long warning times.

6.4. Very catastrophic fragmentations events

Until now, we have assumed that a mitigation mission delivering 500j/kg was causing a disruption with f_r=0.5. Clearly, if 500 j/kg is above the specific energy for barely catastrophic disruption Q^*, we should expect higher levels of fragmentation of the asteroid. As seen in Fig. 13, higher levels of disruption would

spawn a smaller number of dangerous fragments, thus reducing the damage ratio. Another interesting possible scenario would be using much higher levels of collisional energy with the solely purpose to fragment the threatening object providing higher levels of dispersion. In order to analyse these new scenarios, two additional disruption fractions were used f_r=0.25 and f_r=0.1, together with two more collisional energies, 1000 j/kg and 5000 j/kg.
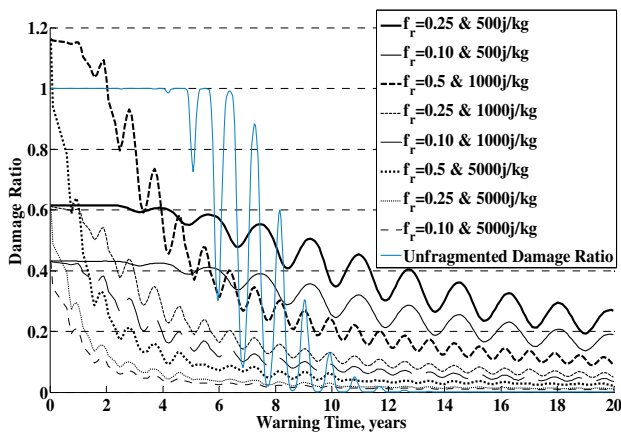
Fig. 17: Damage ratios for a collisional energy of 500 j/kg with disruption levels at f_r=0.25 and f_r=0.1, and collisional energies of 1000 j/kg and 5000 j/kg with disruption levels at f_r=0.5, f_r=0.25 and f_r=0.1.

Fig. 17 show 8 different scenarios with higher disruption levels and higher collisional energies. A kinetic impactor with $m_{s/c}$ of 20,000kg could provide 1000j/kg of SKE to *Apophis* with an impact velocity around 50km/s. Whereas to achieve 5000j/kg of SKE keeping the relative impact velocity of the impactor around 50km/s, i.e., velocities that are achievable with retrograde orbits, the mass of the kinetic impactor should be higher than 70,000kg. Although such an impact mass is highly improbable, a nuclear interceptor could provide the same level of energy with only a 1,000kg of spacecraft dry mass (mass of the spacrecraft without considering propellant), providing the similar change in velocity that a kinetic impactor with 70,000kg.

7. CONCLUSIONS

This work examined the risk of fragmentation that impulsive asteroid deflection mission, such as the kinetic impactor or the nuclear interceptor, can cause when attempting to deflect an asteroid in a single impulsive manoeuvre. A fragmentation and dispersion model was used to analyse the evolution of fragments for up to 20 years after the break-up of the asteroid. Using the probability that five different fragment sizes could impact with the Earth and the number of expected fragments resulting from a catastrophic break-up of *Apophis*, the consequences of a fragmentation were also studied for several illustrative examples.

The energies required for a single impulsive deflection manoeuvre, i.e, those of a kinetic impactor or nuclear interceptor, are dangerously close to the energies required to catastrophically disrupt an asteroid. Even for relatively large warning times, more than 10 years prior to the collision, the risk of fragmentation seems considerable.

If an undesired fragmentation of the threatening object occurs, the risk to Earth is very high. For example, if a fragmentation is triggered while attempting to deflect an asteroid similar to *Apophis*, 10 years prior to the collision, about half the total potential damage of the unfragmented asteroid could be still caused by the few fragments falling onto the Earth. Even if we attempt to fragment the asteroid with five times more energy than the minimum required to fragment an asteroid the damage to Earth is still significant.

8. REFERENCES

[1] Alvarez L.W., Alvarez W., Asaro F. and Michel H.V., "Extraterrestrial Cause for the Cretaceous-Tertiary Extinction," *Science*, Vol. 208, No. 4448, 1980, pp. 1095-1108.

[2] Holsapple K.A., "The Scaling of Impact Processes in Planetary Science," *Annual Review of Earth and Planetary Science,* Vol. 21, 1993, pp. 333-373.

[3] Ryan E.V. and Melosh H.J., "Impact Fragmentation: From the Laboratory to Asteroids," *Icarus*, Vol. 133, No. 1, 1998, pp. 1-24.

[4] Melosh H.J., Nemchinov I.V. and Zetzer Y.I., "Non-nuclear Strategies for Deflecting Comets and Asteroids," *Hazard Due to Comets and Asteroids*, edited by T.Gehrels University of Arizona, 1994, pp. 1110-1131.

[5] Ivashkin V.V. and Smirnov V.V., "An Analysis of Some Methods of Asteroid Hazard Mitigation for the Earth," *Planetary and Space Science*, Vol. 43, No. 6, 1994, pp. 821-825.

[6] Remo J.L., "Energy Requirements and Payload Masses for Near-Earth Objects Hazard Mitigation," *Acta Astronautica*, Vol. 47, No. 1, 2000, pp. 35-50.

[7] "Near-Earth Objects Survey and Deflection Analysis of Alternatives," National Aeronautics and Space Administration, NASA Authorization Act of 2005, 2007.

[8] Sanchez J.P., Colombo C., Vasile M. and Radice G., "Multi-criteria Comparison among Several Mitigation Strategies for Dangerous Near Earth Objects," *Journal of Guidance, Control and Dynamics*, to appear, 2008.

[9] Ahrens T.J. and Harris A.W., "Deflection and Fragmentation of Near-Earth Asteroids," *Nature*, Vol. 360, 1992, pp. 429-433.

[10] Stokes G.H., Yeomans D.K., and *et.al.*, "Study to Determine the Feasibility of Extending the Search for Near-Earth Objects to Smaller Limiting Diameters," NASA, 2003.

[11] O'Brien D.P. and Greenberg R., "Steady-state size distributions for collisional populations: analytical solution with size-dependent strength," *Icarus*, Vol. 164, 2003, pp. 334-345.

[12] Holsapple K.A., "Catastrophic disruptions and cratering of solar system bodies: a review and new

results," *Planetary and Space Science*, Vol. 42, No. 12, 1994, pp. 1067-1078.

[13] Harris A.W., "The Rotation Rates of Very Small Asteroids: Evidence for 'Rubble Pile' Structure," *Lunar and Planetary Science*, Vol. 27, 1996, pp. 493.

[14] Chesley S.R. and Spahr T.B., "Earth Impactors: Orbital Characteristics and Warning Times," *Mitigation of Hazardous Comets and Asteroids* 2003.

[15] Vasile M. and Colombo C.. "Optimal Impact Strategies for Asteroid Deflection," *Journal of Guidance, Control and Dynamics*, Vol.31, No.4, 2008.

[16] Tedeschi W.J., Remo J.L., Schulze J.F., and Young R.P., "Experimental Hypervelocity Impact Effects on Simulated Planetesimal Materials," *International Journal of Impact Engineering*, Vol. 17, 1995, pp. 837-848.

[17] McInnes C., "Deflection of Near-Earth Asteroids by kinetics Energy Impacts from Retrograde Orbits," *Planetary and Space Science*, Vol. 52, No. 7, 2004, pp. 587-590.

[18] Petropoulos A.E., Kowalkowski T.D., Vavrina M.A., Parcher D.W., Finlayson P.A., Whiffen G. J. and Sims J.A., "1stACT global trajectory optimisation competition: Results found at the Jet Propulsion Laboratory," *Acta Astronautica*, Vol. 61, 2007, pp. 806-815.

[19] Davis D.R. and Ryan E.V., "On Collisional Disruption: Experimental Results and Scaling Laws," *Icarus*, Vol. 83, No. 156, 1990, pp. 182.

[20] H.Goldstein, *Mecánica Clásica*, 1996, pp. 518-520.

[21] Gault D.E., Shoemaker E. M., and Moore H.J., "Spray Ejected from the Lunar Surface by Meteoroid Impact," NASA Technical Note D-1767, 1963.

[22] Wiesel W., "Fragmentation of Asteroids and Artificial Satellites in Orbit," *Icarus*, 1978, pp. 99-116.

[23] Greenberg R., Wacker J.F., Hartmann W.K., and Chapman C.R., "Planetesimal to Planets: Numerical Simulations of Collisional Evolution," *Icarus*, Vol. 35, 1978, pp. 1-26.

[24] Mizutani H., Takagi Y. and Kawakami S.I., "New Scaling Laws on Impact Fragmentation," *Icarus*, Vol. 87, 1990, pp. 307-326.

[25] Hills J.G. and Goda M.P., "The Fragmentation of Small Asteroids in the Atmosphere," *The Astronomical Journal*, Vol. 105, No. 3, 1993, pp. 1114-1144.

[26] Chesley S.R. and Ward S.N., "A Quantitative Assessment of the Human and Economic Hazard from Impact-generated Tsunami," *Natural Hazards*, Vol. 38, 2006, pp. 355-374.

[27] Chapman C.R. and Morrison D., "Impacts on the Earth by asteroids and comets: assessing the hazard," *Nature*, Vol. 367, 1994, pp. 33-40.